

Optimum actuator placement for damping of vibrations using the Prestress–Accumulation Release control approach

Blazej Poplawski, Grzegorz Mikułowski, Dominik Pisarski,
Rafał Wiszowaty and Łukasz Jankowski*

*Institute of Fundamental Technological Research, Polish Academy of Sciences,
ul. Pawińskiego 5B, 02-106 Warsaw, Poland*

(Received keep as blank , Revised keep as blank , Accepted keep as blank)

Abstract. This paper proposes and tests a quantitative criterion for optimization of actuator placement for the Prestress–Accumulation Release (PAR) strategy of mitigation of vibrations. The PAR strategy is a recently developed semi-active control approach that relies on controlled redistribution of modal vibration energy into high-order modes, which are high-frequency and thus effectively dissipated by means of the natural mechanisms of material damping. The energy transfer is achieved by a controlled temporary removal of selected structural constraints. This paper considers a short-time decoupling of rotational degrees of freedom in a frame node so that the bending moments are temporarily not transferred between the involved beams. If such a decoupling is performed at a local maximum of the bending strain energy of adjacent beams, it results in an almost instantaneous energy release into high-frequency local vibrations, and consequently, in a quick dissipation of energy. We propose and test a quantitative criterion for placement of such actuators. The criterion is based on local modal strain energy that can be released into high-order modes. The numerical time complexity is linear with respect to the number of actuators and potential placements, which facilitates quick analysis in case of large structures.

Keywords: semi-active control; damping of vibrations; actuator placement; smart structures; Prestress–Accumulation Release (PAR)

1. Introduction

In the recent two decades, a significant stream of research has emerged that focuses on semi-active control in structural and mechanical engineering (Hurlebaus and Gaul 2006; Spencer Jr and Nagarajaiah 2003; Holnicki-Szulc *et al.* 2015). The crucial characteristics of semi-active systems, the ones that clearly differentiate them from active control systems and passive systems, is their smart self-adaptivity and low consumption of energy, which is used for adaptive modification of selected structural properties rather than for exerting significant control forces. Available research publications grow in number and are widely diversified: they consider variable stiffness devices (Karami *et al.* 2016), semi-active tuned mass dampers (Soria *et al.* 2017), mitigation of vibrations in space structures (Mroz *et al.* 2015; Zhan *et al.* 2017) or in coupled electro-mechanical systems (Michajłow *et al.* 2017), adaptive landing gears (Mikułowski and Jankowski 2009), tracks under moving loads (Pisarski 2018a), crashworthiness of vehicles (Griskevicius *et al.* 2007) and thin-walled structures (Graczykowski and Holnicki-Szulc 2015), etc.

*Corresponding author, Assoc. Prof., E-mail: ljank@ippt.pan.pl

Besides relatively widely studied systems with one degree of freedom (Dof) and vibration damping based on adjustable stiffness (Liu *et al.* 2005; Onoda *et al.* 1990), a relatively significant part of the published research concerns approaches based on semi-active energy management, either kinetic impact energy (Faraj *et al.* 2016) or strain/potential energy of the structural vibrations (Mróz *et al.* 2015; Marzec and Holnicki-Szulc 1998). The latter approaches aim at the management and dissipation of the vibration energy contained in lightly-damped, low-frequency structural modes. Most of them focus on the example of a cantilever beam composed of two detachable layers in its fundamental vibration mode, and differ in the applied control technologies: magnetorheological elastomers (Szmidski *et al.* 2017), truss-frame nodes (Mróz *et al.* 2015), granules jammed with underpressure (Bajkowski *et al.* 2016), controllable delamination (Mróz *et al.* 2010), etc. Recently, they have been extended to a decentralized control approach applicable to general frame structures and vibration patterns (Pisarski 2018b; Poplawski *et al.* 2018). However, the placement of actuators in such applications has not been formally investigated so far: it is usually decided ad hoc and based on common engineering sense. Here, we study the problem of optimum placement of actuators for the recently proposed and experimentally verified on/off decentralized semi-active control strategy (Poplawski *et al.* 2018). We propose a quantitative and numerically effective criterion based on local modal strain energy. Its effectiveness is demonstrated in a thorough numerical experiment by regressing the effectiveness obtained in actual transient analysis with respect to the value of the proposed criterion and assessing the coefficient of determination R^2 . The numerical time complexity of the proposed criterion is linear with respect to the number of potential placements, which facilitates planned applications to large structures, including modular structures (Zawidzki and Jankowski 2018) and wide-span skeletal roofs (Wilde *et al.* 2013), as well as to mitigation and monitoring of traffic-induced vibrations (Zhang *et al.* 2013).

The paper is structured as follows. The following Sections 2 and 3 describe respectively the very idea of semi-active control by means of structural constraints and the recently introduced control algorithm that utilizes truss-frame nodes with controllable ability to transfer moments (Poplawski *et al.* 2018). The quantitative criterion for optimization of placement of such nodes is proposed in Section 4 and then thoroughly verified and illustrated in a numerical example in Section 5.

2. Semi-active control using structural constraints

One of the common traits in the recent research stream on practical applications of the semi-active control, which can be traced back to the switchable-stiffness truss elements proposed in 1990s (Onoda *et al.* 1990), and which progressed then to controllable delamination (Mróz *et al.* 2010), jammed granular material (Bajkowski *et al.* 2016) and nodes with controllable ability to transfer moments (Mróz *et al.* 2015; Poplawski *et al.* 2018), can be identified as *controllable structural constraints*. In all these works, the transfer and dissipation of vibration energy have been effectively achieved by controlled removal of properly selected structural constraints (Marzec and Holnicki-Szulc 1998).

A typical example is the short-time decoupling of rotational degrees of freedom in a frame node, which has been proposed and studied numerically in Mróz *et al.* (2015) and then experimentally in Poplawski *et al.* (2018): in the result of such a decoupling, the bending moments are, for a short time, no longer transmitted between the adjacent beams, and the node acts

effectively as a hinge. In practice, such nodes can be friction-based and controlled by an actuator that exerts a normal force of a controllable level (Gaul et al. 1998; Gaul and Nitsche 2001). Development and verification of control algorithms require a formal model of such a node. Three general approaches can be used for that purpose:

1. A physically accurate approach would be to model the dry friction; it could be also readily implemented in commercial finite element (FE) software packages (Mróz *et al.* 2015). However, the resulting nonlinearity of the structural model makes it difficult to be theoretically analyzed using typical tools aimed at linear dynamics.
2. Two models of the actuator can be assembled and incorporated into the structural model: a model with the constraint activated (a frame-like model of the node) and a model without the constraint (a truss-like model of the node). During the simulation, the on/off control process can be implemented by switching the local modes of the actuators, in an approach that resembles switching control systems (Liberzon 2003). Such an approach preserves the linearity of the system in-between the switching instances. It can be also used to accurately model the ideal truss-frame node with its either infinite or zero (on/off) ability to transfer moments. However, the model of the global structural changes in each switching instance, and the changes include the effective number of Dofs, which hinders theoretical analysis and makes numerical simulations difficult.
3. To avoid the theoretical difficulties related to either nonlinearity or model-switching, we have recently proposed a third approximate approach suitable for transient analysis (Popławski *et al.* 2018). The approach uses a single linear structural model throughout the entire analysis, and the controllable constraints are implemented in the form of a bilinear control.

Here, the third approach is used. The frame model is used for the entire structure; however, a larger number of rotational Dofs is used in each controllable node. These Dofs remain distinct and are not aggregated into a single Dof in the structural matrices. The control is modelled as a controllable involvement/removal of the constraint $\dot{\theta}_1 = \dot{\theta}_2$, which effectively blocks/unblocks the relative rotations of the involved Dofs and thus enables/disables the transfer of moments between involved adjacent beams. Such an approach is implemented in an approximate and numerically efficient bilinear form, that is through modifications of the viscous damping of the relative rotations in the non-aggregated Dofs. A high relative damping effectively couples the respective Dofs and allows the moments to be transferred. The equation of motion of the controlled structure takes thus the following form:

$$\mathbf{M}\ddot{\mathbf{x}}(t) + (\mathbf{C} + \sum_{i=1}^N \gamma_i(t)\mathbf{C}_i)\dot{\mathbf{x}}(t) + \mathbf{K}\mathbf{x}(t) = \mathbf{f}(t), \quad (1)$$

where $\mathbf{f}(t)$ is the external excitation and \mathbf{M} , \mathbf{C} and \mathbf{K} denote the mass, damping and stiffness matrices of the structure with unaggregated rotational Dofs in the controllable nodes. In each controllable node the rotational Dofs are coupled using the matrix \mathbf{C}_i , and $\gamma_i(t)$ is the respective control function, which is of the bang-bang type, that is $\gamma_i(t) \in \{0, \gamma_i^{\max}\}$. The Dofs are effectively decoupled when $\gamma_i(t) = 0$, while the node is at its maximum ability to transmit moments when $\gamma_i(t) = \gamma_i^{\max}$. In the transient analysis and for large γ_i^{\max} , the model has been shown in Popławski *et al.* (2018) to be equivalent to the standard frame model of the structure.

3. Decentralized prestress–accumulation release (PAR) strategy

The prestress–accumulation release (PAR) approach is a recently proposed semi-active on/off control strategy aimed at mitigation of structural vibrations (Mróz *et al.* 2010, 2015; Poplawski *et al.* 2018). The core idea is the redistribution of modal energy and effective utilization of structural vibration modes (Wierschem 2017). The aim is to transfer the vibration energy, in a controlled way, from low-frequency, lightly damped fundamental vibration modes into high-frequency high-order modes, where it is effectively and quickly dissipated by means of natural mechanisms of material damping.

The energy transfer is achieved by a controlled removal of selected structural constraints. The examples studied so far involved controllable delamination and the truss-frame nodes described in the previous section. Numerical models included the physically exact dry friction model implemented in a commercially available FE package and the described approximate viscous coupling. For the purpose of experimental verification, dry friction based joints have been used, driven by piezoelectric stack actuators.

In their standard (passive or power-failure) state, the controllable nodes are in their “on” state, that is they transmit the moments between adjacent beams and the respective rotational Dofs are coupled. A short-time switching to the “off” state turns the nodes temporarily into hinges and decouples the rotational Dofs. If such a decoupling is performed at the maximum of the bending strain energy of the adjacent beams, it results in an almost instantaneous energy release into high-frequency local vibrations and quick dissipation. Based on such an idea, the following simple decentralized algorithm has been recently proposed and numerically and experimentally verified to be extremely effective in mitigation of free vibrations of 2D frame structures (Poplawski *et al.* 2018): The i th controllable node (or a synchronously controlled group of nodes) is controlled based on the local feedback signal $E_i(t)$, which quantifies the local bending energy that can be released by decoupling the relative rotations of the involved Dofs and which in practice is proportional to strain gauge measurements. The controllable node(s) start the operation in their frame-like passive configuration (“on” state, maximum ability to transmit moments). The state-switching time points are decided based on the local feedback signal $E_i(t)$ as follows:

1. The node(s) stay in their frame-like mode (“on” state, full transmission of moments) as long as $E_i(t)$ increases.
2. When $E_i(t)$ attains its local maximum, the node(s) switch to the truss-like mode (“off” state, no transmission of moments) and stay so for a short time interval t_0 .
3. Then, the node(s) switch back to the frame-like mode (“on” state, transmission of moments restored).

Finally, the node(s) wait again for the next maximum of the local energy measure $E_i(t)$, so that the above control sequence is repeated iteratively. Upon switching to the truss-like mode (“off” state) in step 2, the accumulated strain energy is released into high-frequency local vibrations. The time t_0 should be long enough to ensure that these vibrations decay and the released energy is dissipated. The exact value of t_0 is in practice not crucial, as the control algorithm has been tested to stay effective for a wide range of its values.

In earlier works (Mróz *et al.* 2015), a cantilever beam-like structure in its fundamental vibration mode has been considered with all the controllable nodes operated synchronously. The local $E_i(t)$ has been approximated by a global displacement of the cantilever tip, which has been assumed for control purposes to represent the global structural potential energy. In the algorithm described above, the feedback signal $E_i(t)$ quantifies the local bending energy, which allows the algorithm

to operate in a decentralized manner and to apply at the local level the originally global prestress-accumulation release (PAR) control concept. As a result, it allows the PAR strategy to be applied with more complex vibration patterns and structures, which calls for a quantitative approach to actuator placement.

4. Quantitative criterion for actuator placement

In Poplawski *et al.* (2018), the placement of controllable nodes has been selected ad hoc, based on common engineering sense. In this section, we propose a single quantitative measure that allows various possible placements of such node(s) to be consistently assessed irrespective of the total number of the used controllable nodes. In active control systems, the problem of optimum placement of actuators is well-researched (Friswell and Mottershead 1995; Gupta *et al.* 2010; Fesharaki and Golabi 2016). However, in the case of semi-active control systems, the problem seems to be relatively unexplored. The criterion proposed here is based on two intuitive observations:

1. The more a beam element is bent, the more energy it can release into local vibrations upon removing the constraints imposed on the rotation of its ends.
2. One should focus on mitigation of low-order modes since as opposed to higher-order modes, they are lightly damped and thus contribute to energy dissipation in a negligible degree.

Therefore, we propose here to quantify placements of nodes separately with respect to each target low-order vibration mode. The decisive factor is the bending energy of the adjacent beams that can be released into local vibrations by removing the constraint.

4.1 Nodes operated independently

In the general case, the placement of the i th node is quantified with respect to the k th mode by the relative local strain energy E_{ik} that can be released upon switching the node to the “off” state. Such a measure coincides with the local feedback signal E_i recalled in Section 3 (computed for the structure in its k th modal shape), which has been shown in Poplawski *et al.* (2018) to be expressible in terms of intrinsically local quantities as follows:

$$E_{ik} = 2 \sum_j \frac{\left(\sum_{b \in B_{ij}} \frac{EI_b}{h_b} \varepsilon_{bik} \right)^2}{\sum_{b \in B_{ij}} \frac{EI_b}{\eta_{bi} L_b}}, \quad (2)$$

where i indexes the controllable nodes, k is the mode number, j indexes the rotational Dofs of the i th node, B_{ij} denotes the set of the beams aggregated to the j th rotational Dof of the i th node, EI_b , h_b and L_b denote the structural and geometric parameters of the beam b (bending stiffness, height and length), ε_{bik} denotes the (curvature-related component of the) strain measured locally near the i th controllable node at in the k th (energy-normalized) modal shape, and $\eta_{bi} \in \{2,3\}$ is a parameter related to the type of the rotational boundary conditions on the other end of the beam b (fixed or free).

4.2 Nodes operated pairwise

In the specific case considered in Poplawski *et al.* (2018), the controllable nodes were placed pairwise on two ends of selected beams and operated synchronously. The local potential energy that can be released by simultaneous activation of such a pair of nodes can be treated as proportional to the bending/shear strain energy of the involved beam,

$$E_{ik} = \frac{1}{2} \boldsymbol{\varphi}_k^T \mathbf{L}_i \mathbf{K}_i \mathbf{L}_i^T \boldsymbol{\varphi}_k, \quad (3)$$

where i denotes the involved beam, $\boldsymbol{\varphi}_k$ is the k th global modal vector (energy-normalized to 1), \mathbf{L}_i is the local-to-global transformation matrix, and \mathbf{K}_i is the local stiffness matrix of the i th beam that involves only the rotational and transverse displacement Dofs of the beam.

4.3 Mode controllability index

Equations (2-3) define a mode controllability index E_{ik} for a single mode k and a single controllable node/beam i . In practice, a number of low-order nodes can be excited and should be treated as target modes and mitigated. Similarly, several controllable nodes might be available for application. Therefore, instead of single k and i , there is $k \in \mathcal{B}$ and $i \in \mathfrak{S}$. In such a case, we propose to quantify the placements by summing the controllability indices for successive placements i and then taking the root means square value with respect to the considered modes k ,

$$E_{\mathfrak{S}\mathcal{B}} := \text{rms}_{k \in \mathcal{B}} \sum_{i \in \mathfrak{S}} E_{ik}, \quad (4)$$

which expresses the fact that each node/beam contributes to the transfer of energy. In practice, the higher the mode order, the harder it is to mitigate, so that the criterion tends in applications to be biased towards higher-order and hardest-to-damp among the set \mathcal{B} of the target modes. Notice that larger values of the controllability index $E_{\mathfrak{S}\mathcal{B}}$ denote better placements.

4.4 Optimization problem

Given the set \mathfrak{S} of the target modes and the set \wp of all possible placements of actuators, the aim of optimization is to maximize $E_{\mathfrak{S}\mathcal{B}}$, where the optimization variable is the set $\mathcal{B} \in \wp$ of actuator placements:

$$\begin{aligned} & \text{maximize } E_{\mathfrak{S}\mathcal{B}} \\ & \text{subject to } \mathcal{B} \in \wp. \end{aligned} \quad (5)$$

Even though the domain \wp and thus the entire optimization procedure has a discrete character, the proposed formulation is numerically very effective. The most costly operation is the computation of the modal shapes and then the computation of the individual indices E_{ik} according to Eq. (2) or Eq. (3), but these are the costs of a standard modal analysis. Thereupon, given the individual indices, computation of $E_{\mathfrak{S}\mathcal{B}}$ according to Eq. (4) is linear with respect to the number of considered controllable nodes/beams (allowable actuator positions), as well as with respect to the number of the considered modes. In other words, to find the best placement of n actuators out of m allowable positions, it is enough just to find the n largest values of the index $E_{\mathfrak{S}\mathcal{B}}$, which can be found in time $O(nm)$. Moreover, optimization of actuator placement requires simple matrix operations that are straightforwardly parallelizable and can be performed without any repeated structural analysis.

5. Numerical example

This example tests and illustrates the proposed actuator placement criterion using the numerical example of a 2D frame structure, which is similar to the example presented in Poplawski *et al.* (2018). However, the placement of the actuators is no longer decided ad hoc but rather selected according to the proposed criterion. The proposed criterion is verified by assessing the coefficient of determination in a regression analysis of the actual effectiveness obtained in transient tests.

5.1 The structure and the target modes

Figure 1 depicts the 2D frame structure used in the example. The frame is made of steel beams with 1 mm x 1 mm cross-sections. The total dimensions are 1 m x 0.1 m. Young's modulus is 200 GPa and the density equals 7850 kg/m³. The two left-hand side nodes are fixed. A stiffness-proportional damping model is used with 1% critical damping ratio for the first mode.

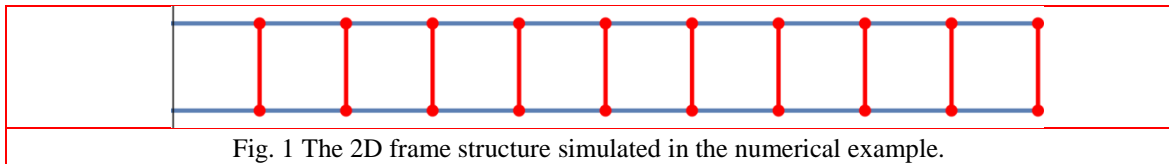


Fig. 1 The 2D frame structure simulated in the numerical example.

It is assumed that higher-order vibration modes are effectively damped by natural mechanisms of material damping. Consequently, the analysis is focused on low-order lightly-damped modes with the critical damping ratio below 10%. There are four such modes, which are typical cantilever beam type modes with natural frequencies that equal respectively 6.1 Hz, 18.7 Hz, 32.3 Hz, 47.4 Hz and the critical damping ratios respectively equal 1.0%, 3.1%, 5.3% and 7.7%. The modes are illustrated in Fig. 2.

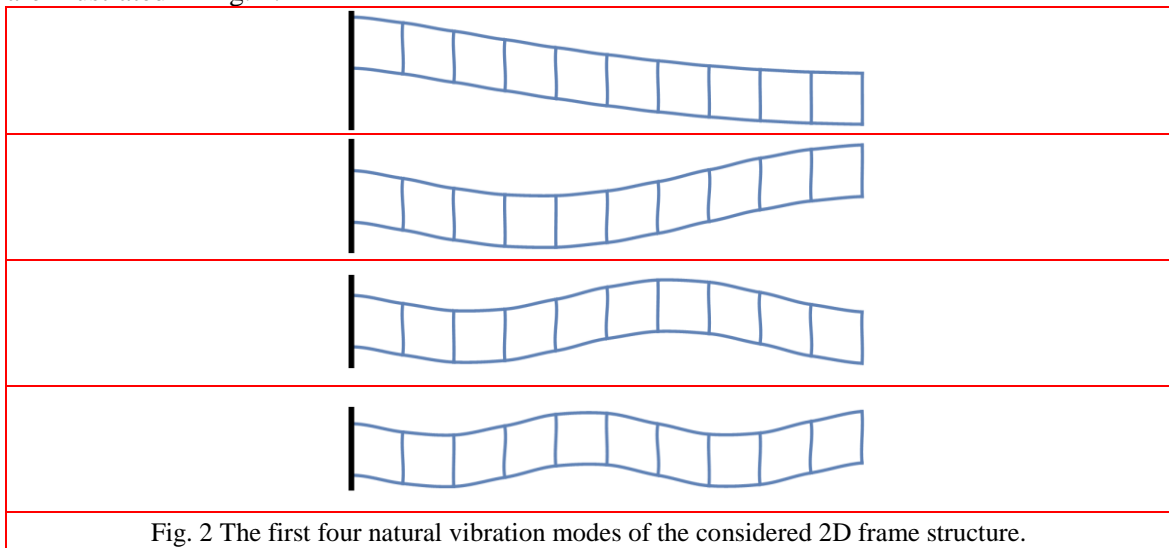


Fig. 2 The first four natural vibration modes of the considered 2D frame structure.

5.2 Placements of controllable nodes

As a result of the symmetry of the structure and of the considered vibration modes, the controllable nodes are placed pairwise in both ends of selected vertical beams (marked red in Fig. 1), which in the following are numbered from 1 to 10 (left to right). Consequently, Eq. (3) is used to express mode controllability indices E_{ik} for individual modes and placements. It is assumed that one up to five beams can be instrumented: the set \wp contains thus all 1- to 5-element subsets of the set $\{1,2,\dots,10\}$. There is a total of 637 potential actuator placements, which is a number high-enough for a regression analysis.

In the following, for graphical representation of the placements $\mathcal{B} \in \wp$, strings of “○” and “-” are used, 10 characters in total, where each character corresponds to a single beam (a pair of controllable nodes). For example, the string “○-○-----” is used to encode that two vertical beams (No 1 and No 3) are instrumented with controllable nodes.

5.3 Assessment criterion

For each considered placement of the controllable nodes, the corresponding effectiveness of the decentralized damping algorithm is verified by performing eight transient free vibration tests. Initial displacement conditions are used, and the initial displacement vectors correspond to the four considered modes, see Section 5.1. For each mode $i \in \mathfrak{S}$, two tests are performed: the reference passive test (no control, nodes in the passive “on” state with full transmission of moments) and the test with the control algorithm activated (using the tested actuator placement). Finally, for the entire set of considered target modes \mathfrak{S} , the normalized effectiveness measure is defined as the root mean square value of the ratio of the total energy integrals (controlled to the passive case),

$$\zeta_{\mathfrak{S}\mathcal{B}} := \text{rms}_{i \in \mathfrak{S}} \frac{\int_0^T E_{i\mathcal{B}}^{\text{controlled}}(t) dt}{\int_0^T E_{i\mathcal{B}}^{\text{passive}}(t) dt}, \quad (6)$$

where $E_{i\mathcal{B}}^{\text{controlled}}(t)$ and $E_{i\mathcal{B}}^{\text{passive}}(t)$ denote the computed time evolutions of the total structural energies (potential + kinetic) in the controlled and passive tests, respectively. The index $i \in \mathfrak{S}$ denotes the target mode that is used as the initial displacement condition, and the set \mathcal{B} denotes the assessed placement of the controllable nodes. Notice that a lower value of $\zeta_{\mathfrak{S}\mathcal{B}}$ means a better effectiveness and better actuator placement. This is opposite to the proposed criterion $E_{\mathfrak{S}\mathcal{B}}$, which is the higher the better.

In general, we verify the proposed mode controllability index by plotting the assessment index $\zeta_{\mathfrak{S}\mathcal{B}}$ versus the proposed mode controllability index $E_{\mathfrak{S}\mathcal{B}}$ for a number of possible actuator placements. Then, we perform a (nonlinear) regression and assess the coefficient of determination R^2 (the ratio of the variance of $\zeta_{\mathfrak{S}\mathcal{B}}$ explained by $E_{\mathfrak{S}\mathcal{B}}$ to the total variance of $\zeta_{\mathfrak{S}\mathcal{B}}$). High values of R^2 attest that the proposed criterion is reliable, that is it properly quantifies the actual performance of the assessed actuator placements.

Notice that several full transient simulations of the entire structure are required in order to compute Eq. (6), which is very different in nature and much more time-consuming than the proposed simple measure of Eq. (4). We propose thus to select the placement of the actuators using the simple to use criterion Eq. (4). Then, we justify the proposed criterion in this numerical example by using Eq. (6) and performing a number of full transient analyses.

In the tests, the total simulation time T is 1 s, and the half-cycles (periods of “off” or “on” states)

are not shorter than 1 ms, which corresponds to limiting the maximum switching frequency at the level of 500 Hz.

5.4 Verification results

All the tests are performed for four sets of target modes:

$$\mathfrak{S}_1 = \{1\}, \quad \mathfrak{S}_2 = \{1,2\}, \quad \mathfrak{S}_3 = \{1,2,3\}, \quad \mathfrak{S}_4 = \{1,2,3,4\}. \quad (7)$$

The 637-element set \wp of considered actuator placements is explained in Section 5.2. For each of the four sets \mathfrak{S}_n , $n = 1, \dots, 4$, a set of 637 pairs

$$\{(E_{\mathfrak{S}_n \mathcal{B}}, \zeta_{\mathfrak{S}_n \mathcal{B}}) | \mathcal{B} \in \wp\} \quad (8)$$

is computed by performing transient tests as described in Section 5.3. Figure 3 presents the point plots of the four sets obtained this way along with a strictly decreasing nonlinear regression curve given by

$$\zeta_{\mathfrak{S}_n \mathcal{B}} \sim c_1 + \frac{c_2}{c_3 + E_{\mathfrak{S}_n \mathcal{B}}} \quad (9)$$

and the corresponding coefficient of determination R^2 .

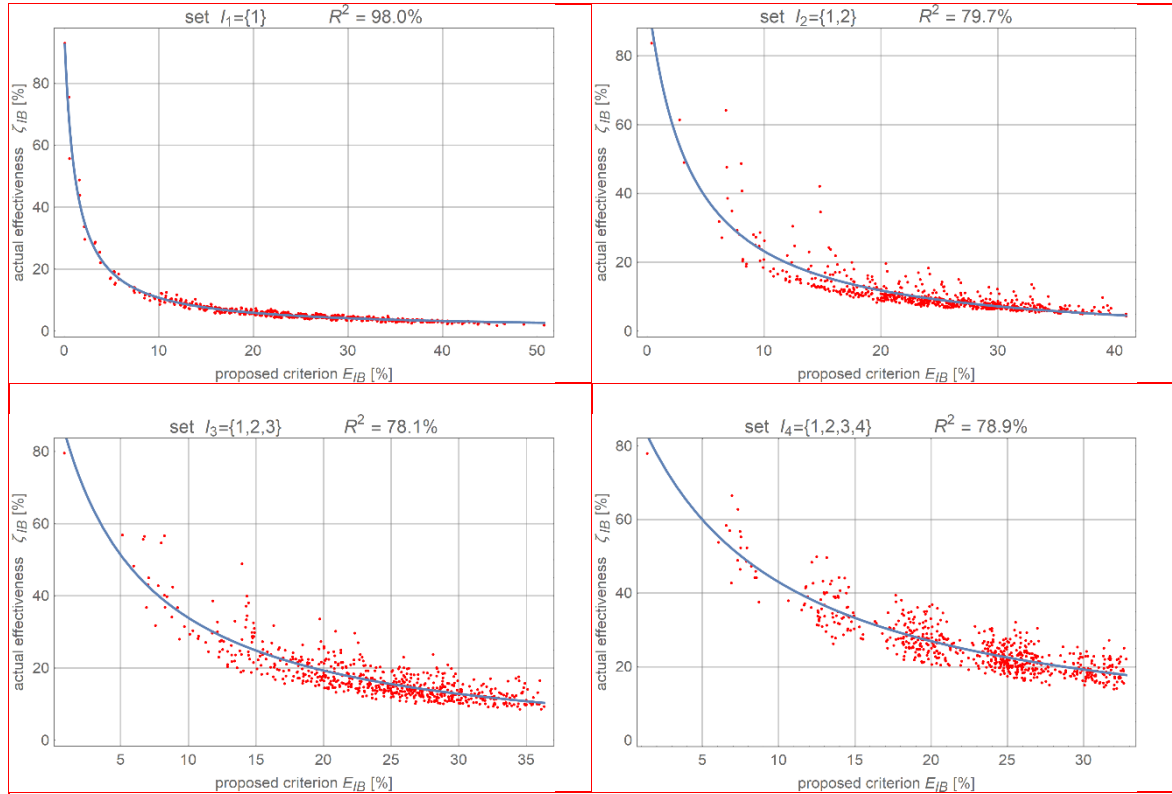


Fig. 3 Actual effectiveness of assessed actuator placements versus the proposed criterion for the four considered sets of target modes: point plots and the regression lines.

The coefficients of determination R^2 range from 78% (for the sets \mathfrak{S}_2 , \mathfrak{S}_3 and \mathfrak{S}_4) to 98% (for a single target mode, that is the set \mathfrak{S}_1). Consistently high values of R^2 attest that the proposed assessment criterion reliably explains the major part of the variance of the actual effectiveness of the tested actuator placement.

5.5 Optimization examples

To illustrate the usage of the proposed and tested criterion, individual indices E_{ik} are computed separately, according to Eq. (3), for the first four modes, $k \in \{1,2,3,4\}$, and for each vertical beam, $i \in \{1,2, \dots, 10\}$. Since all vertical beams are the same, the computed values are a (quadratic) measure of the bending/shear strain of the individual beams in the modal shapes illustrated in Fig. 2. These values are then used to compute the indices $E_{\mathfrak{S}_4\mathcal{B}}$, and to find the three best and worst placements of one to five instrumented beams with respect to the target modes 1–4. Table 1 lists some of the best and worst placements.

Table 1 Best and worst placements of actuators with respect to modes 1–4 and according to Eqs. (3)-(4)

	Modes 1–4 best	Modes 1–4 worst
1 beam	○----- -----○--- -----○--	-----○ -----○--- -----○-
2 beams	○-----○-- ○----○---- ○-○-----	----○----○ -○-----○ -----○--○
3 beams	○-○--○---- ○-○○----- ○----○-○--	-○-----○○ ----○-○--○ ---○--○--○
4 beams	○----○○○-- ○○○--○---- ○○○○-----	-○--○--○○ -○----○-○○ ----○-○-○○
5 beams	○○○○-○---- ○○○○○----- ○-○○-○-○--	-○--○-○-○○ -○-○--○-○○ -○○--○-○○

For illustration purposes, the case of the best and worst placement of three instrumented beams is selected. The corresponding values of the indices are as follows:

$$(E_{\mathfrak{S}_4\{1,3,6\}}, \zeta_{\mathfrak{S}_4\{1,3,6\}}) = (21.0, 27.4), \quad (E_{\mathfrak{S}_4\{2,9,10\}}, \zeta_{\mathfrak{S}_4\{2,9,10\}}) = (11.7, 36.7) \quad (10)$$

Fig. 4 plots the time histories of the vertical displacement of the frame (right-hand side) tip for the passive case and the two corresponding semi-actively controlled cases. In the four subfigures, the initial displacement conditions correspond respectively to the first four modes of natural vibrations. Three cases are depicted in each subfigure:

1. The reference passive case with no control (black line);
2. Semi-active control with beams No 1, 3 and 6 instrumented (blue line), which is the best placement as listed in Table 1;
3. Semi-active control with beams No 2, 9 and 10 instrumented (yellow line), which is the worst placement as listed in Table 1.

The effectiveness of the control algorithm, as well as the beneficial effects of proper placement of actuators, can be observed. It can be also noted that the effects of the proper placement of actuators are most clear for first target mode, as well as for the highest-order fourth target mode. The latter is an expected consequence of the fact that the fourth mode is the hardest-to-mitigate target mode.

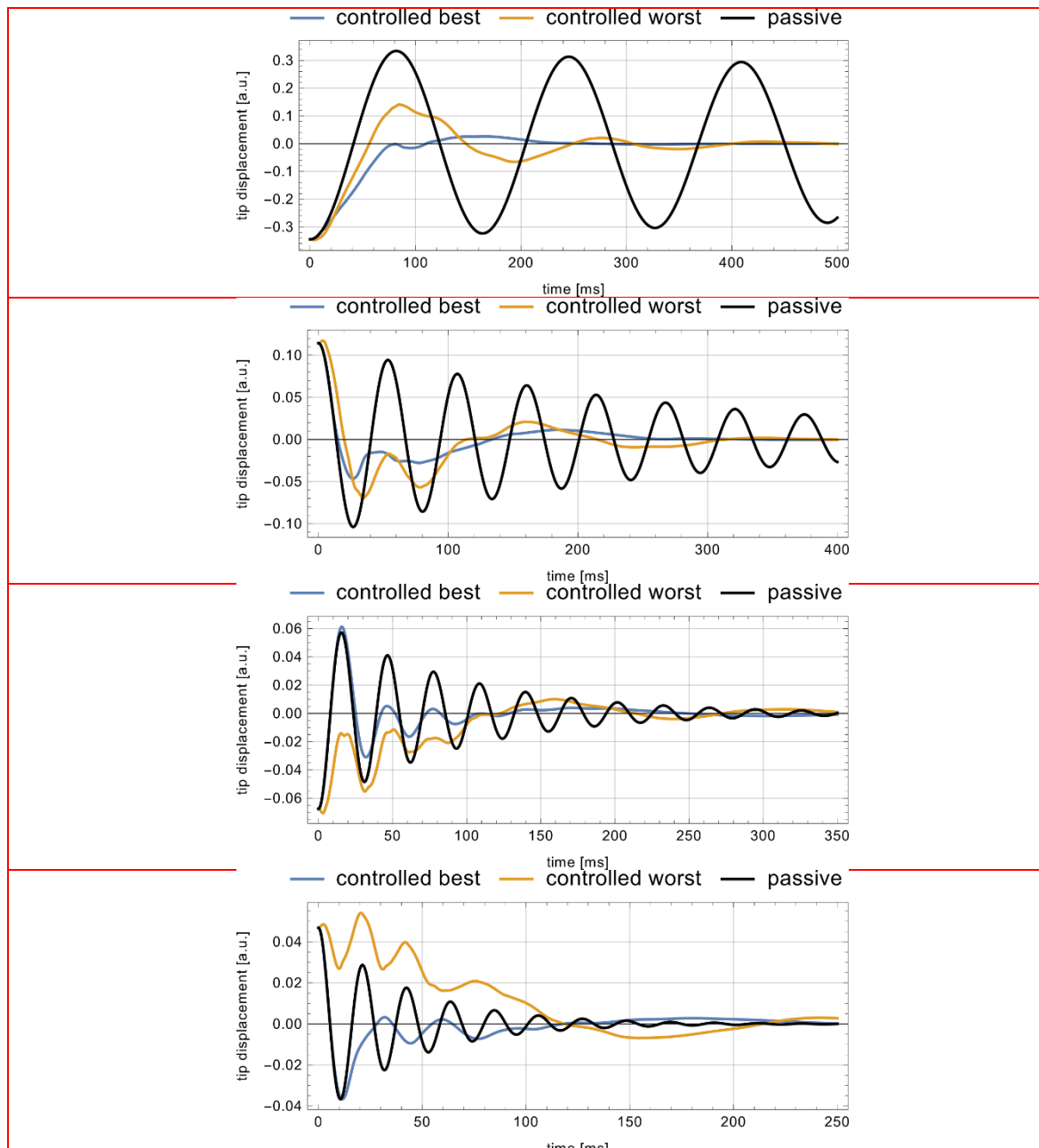


Fig. 4 Vertical displacements of the frame right-hand-side tip for the initial displacement conditions equal to the four initial modes. Passive case (black line) compared to two semi-actively controlled cases with three instrumented beams placed in the best (blue line) and worst positions (yellow line).

6. Conclusions

This contribution proposes, tests and verifies a quantitative criterion for optimization of actuator placement, to be used with the prestress–accumulation release (PAR) semi-active control strategy. The criterion requires modal indices to be computed for the potential placements, which in numerical terms is equivalent to performing a modal analysis of the involved structure. Given the modal indices, the optimization relies on simple and easily parallelizable matrix operations, without the need for any transient simulation or analysis.

Low numerical cost of the optimization facilitates planned further research on the application of the PAR strategy to damping of large and complex 3D skeletal structures, including modular structures, wide-span skeletal roofing systems and to traffic-induced vibrations.

Acknowledgments

The authors gratefully acknowledge the support of the National Science Centre, Poland, granted under grant agreements DEC-2017/25/B/ST8/01800 and DEC-2017/26/D/ST8/00883.

References

- Bajkowski, J.M., Bajer, C.I., Dyniewicz, B. and Pisarski, D. (2016), “Vibration control of adjacent beams with pneumatic granular coupler: an experimental study”, *Mechanics Re-search Communications*, **78**, 51–56.
- Faraj, R., Holnicki-Szulc, J., Knap, L. and Senko, J. (2016), “Adaptive inertial shock-absorber”, *Smart Materials and Structures*, **25**, 035031.
- Fesharaki, J. and Golabi, S. (2016), “A novel method to specify pattern recognition of actuators for stress reduction based on particle swarm optimization method”, *Smart Structures and Systems*, **17**(5), 725–742.
- Friswell, M. and Mottershead, J.E. (1995), “Optimising transducer locations”, Chapter 4.6 in “Finite Element Model Updating in Structural Dynamics”, Kluwer Academic Publishers.
- Gaul, L., Lenz, J. and Sachau, D. (1998), “Active damping of space structures by contact pressure control in joints”, *Journal of Structural Mechanics*, **26**(1), 81–100.
- Gaul, L. and Nitsche, R. (2001), “The role of friction in mechanical joints”, *Applied Mechanics Reviews*, **54**, 93–106.
- Griskevicius, P., Zeleniakienė, D., Ostrowski, M. and Holnicki-Szulc, J. (2007), “Crash-worthiness simulations of roadside restraint systems”, *Procs. of the 11th Int’l Conf on Transport Means*, Kaunas, October, 282–285.
- Graczykowski, C. and Holnicki-Szulc, J. (2015), “Crashworthiness of inflatable thin-walled structures for impact absorption”, *Mathematical Problems in Engineering*, **2015**, 830471.
- Gupta, V., Sharma, M. and Thakur, N. (2010), “Optimization criteria for optimal placement of piezoelectric sensors and actuators on a smart structure: A technical review”, *Journal of Intelligent Material Systems and Structures*, **21**(2), 1227–1243.
- Holnicki-Szulc, J., Graczykowski, C., Mikułowski, G., Mróz, A., Pawłowski, P. and Wiszowaty, R. (2015), “Adaptive Impact Absorption—the Concept and Potential Applications”, *International Journal of Protective Structures*, **6**(2), 357–377.
- Hurlebaus, S. and Gaul, L. (2006), “Smart structure dynamics”, *Mechanical Systems and Signal Processing*, **20**, 255–281.

- Karami, K., Nagarajaiah, S. and Amini, F. (2016), "Developing a smart structure using integrated DDA/ISMP and semi-active variable stiffness device", *Smart Systems and Structures*, **18**(5), 955–982.
- Liberzon D. (2003), *Switching in Systems and Control*, Birkhäuser Basel.
- Liu, Y., Waters, T.P. and Brennan, M.J. (2005), "A comparison of semi-active damping control strategies for vibration isolation of harmonic disturbances", *Journal of Sound and Vibration*, **280**(1–2), 21–39.
- Marzec, Z. and Holnicki-Szulc, J. (1998), "Strategy of impulse release of strain energy for damping of vibration", *Procs. of NATO Advanced Research Workshop "Smart Structures"*, 111–114.
- Michajłow, M., Jankowski, Ł., Szolc, T. and Konowrocki, R. (2017), "Semi-active reduction of vibrations in the mechanical system driven by an electric motor", *Optimal Control Application and Methods*, **38**(6), 922–933.
- Mikułowski, G. and Jankowski, Ł. (2009), "Adaptive Landing Gear: optimum control strategy and potential for improvement", *Shock and Vibration*, **16**, 175–194.
- Mróz, A., Holnicki-Szulc, J. and Biczuk, J. (2015), "Prestress accumulation-release technique for damping of impact-born vibrations: Application to self-deployable structures", *Mathematical Problems in Engineering*, **2015**, 720236.
- Mroz, A., Orłowska, A. and Holnicki-Szulc, J. (2010), "Semi-active damping of vibrations. Prestress Accumulation-Release strategy development", *Shock and Vibration*, **17**(2), 123–136.
- Onoda, J., Endo, T., Tamaoki, H. and Watanabe, N. (1990) "Vibration suppression by variable-stiffness members", *AIAA Journal*, **29**(6), 977–983.
- Pisarski, D. (2018a), "Optimal control of structures subjected to traveling load", *Journal of Vibration and Control*, **24**(7), 1283–1299.
- Pisarski, D. (2018b), "Decentralized stabilization of semi-active vibrating structures", *Mechanical Systems and Signal Processing*, **100**: 694–705.
- Poplawski, B., Mikułowski, G., Mróz, A. and Jankowski, Ł. (2018), "Decentralized semi-active damping of free structural vibrations by means of structural nodes with an on/off ability to transmit moments", *Mechanical Systems and Signal Processing*, **100**, 926–939.
- Soria, J.M., Diaz, I.M. and Garcia-Palacios, J.H. (2017), "Vibration control of a time-varying model-parameter footbridge: study of semi-active implementable strategies", *Smart Systems and Structures*, **20**(5), 525–537.
- Spencer Jr, B. and Nagarajaiah, S. (2003), "State of the art of structural control", *Journal of Structural Engineering*, **129**(7), 845–856.
- Szmidt, T., Pisarski, D., Bajer, C.I. and Dyniewicz, B. (2017), "Double-beam cantilever structure with embedded intelligent damping block: Dynamics and control", *Journal of Sound and Vibration*, **401**, 127–138.
- Wierschem, N.E., Hubbard, S.A., Luo, J., Fahnstock, L.A., Spencer, B.F., McFarland, D.M., Quinn, D.D., Vakakis, A.F., Bergman, L.A. (2017), "Response attenuation in a large-scale structure subjected to blast excitation utilizing a system of essentially nonlinear vibration absorbers", *Journal of Sound and Vibration*, **389**, 52–72.
- Wilde, K., Miskiewicz, M. and Chroscielewski, J. (2013), "SHM System of the Roof Structure of Sports Arena Olivia", *Procs. of the 9th Int'l Workshop on Structural Health Monitoring (IWSHM)*, Stanford, CA, September, vol. 2, 1745–1752.
- Zawidzki, M. and Jankowski, Ł. (2018), "Optimization of modular Truss-Z by minimum-mass design under equivalent stress constraint", *Smart Structures and Systems*, **21**(6), 715–725.
- Zhan, M., Wang, S.L., Yang, T., Liu, Y. and Yu, B.S. (2017), "Optimum design and vibration control of a space structure with the hybrid semi-active control devices", *Smart Structures and Systems*, **19**(4), 341–350.
- Zhang, Q., Jankowski, Ł. and Duan, Z. (2013), "Simultaneous identification of moving vehicles and bridge damages considering road rough surface", *Mathematical Problems in Engineering*, **2013**, 963424.